Supplementary Material

Thermodynamic Bounds of Terrestrial Water-Energy Coupling and Resiliency in Global Ecosystems

Debasish Mishra[1], Vinit Sehgal[1,2,3], Binayak Mohanty[1]*

[1]Biological and Agricultural Engineering, Texas A&M University, TX 77843, USA
[2]Water Management and Hydrological Science, Texas A&M University, TX 77843, USA
[3] Now at the School of Plant, Environment, and Soil Sciences, Louisiana State University, LA 70801, USA

*Corresponding author: Binayak P. Mohanty (bmohanty@tamu.edu)

Submitted to

Water Resources Research

Contents

Serial No.	Title	Page No.
01	**Table S1**. Signal to Noise ratio (SNR) blending period for the combined Copernicus Climate Change Service (C3S) soil moisture product.	03
02	**Table S2**. Description of surface meteorological (atmospheric), soil and vegetation variables used for quantification of dominant drivers controlling SM-ET coupling and entropy production.	04
03	**Figure S1**. Global seasonal maps of **(a)** proportional duration spent by the pixel in SM drying ($SM_{AIF} < 0$) or SM wetting ($SM_{AIF} > 0$), and **(b)** proportional duration spent by the pixel in atmosphere heating ($ET_{AIF} < 0$) or cooling ($ET_{AIF} > 0$) for four seasons.	05-06
04	**Table S3.** Statistical summary for seasonal Wasserstein distance, WD (-**)** across hydroclimates (IQR - Interquartile Range, SD - Standard Deviation, SE - Standard Error).	07
05	**Figure S2**. Global maps of seasonal slope factor, γ expressed in kg J^{-1} for four seasons, computed using piecewise linear regression.	08
06	**Figure S3**. Global maps of relative time (τ/τ_0) for four seasons.	09
07	**Figure S4**. Global maps of memory timescale (τ), expressed in secs, for four seasons.	10
08	**Table S4.** Statistical summary for seasonal entropy production, Σ^* (10^{-6} J m^{-2} K^{-1}**)** across hydroclimates	11
09	**Table S5.** Statistical summary for seasonal entropy production, Σ^* (10^{-6} J m^{-2} K^{-1}**)** across terrestrial ecosystems	12
20	**Table S6.** Dissipative energy barriers (Δe, 10^{-6} J m^{-2} K^{-1}) between terrestrial ecosystems computed as the difference between median entropy thresholds	13

Table S1. Signal to Noise ratio (SNR) blending period for the combined Copernicus Climate Change Service (C3S) soil moisture product.

Time Period	Passive Sensors	Active Sensors
2010-01-15 to 2011-10-04	AMSR-E, WindSat, SMOS	ASCAT-A
2011-10-05 to 2012-06-30	WindSat, SMOS	ASCAT-A
2012-07-01 to 2015-03-30	SMOS, AMSR2	ASCAT-A
2015-03-31 to 2015-07-20	SMOS, AMSR2, SMAP	ASCAT-A
2015-07-21 to 2020-12-31	SMOS, AMSR2, SMAP	ASCAT-A, ASCAT-B

Table S2. Description of surface meteorological (atmospheric), soil and vegetation variables used for quantification of dominant drivers controlling SM-ET coupling and entropy production.

Variable	Unit	Description
Near-surface air temperature (T_{air})	K	The temperature of air at 2 meters above the surface of land.
Near-surface specific humidity (q)	kg kg^{-1}	The amount of moisture in the air divided by the amount of air plus moisture at that location.
Near-surface wind speed (u_{surf})	m s^{-1}	The horizontal wind speed at a height of 10 meters above the surface of the Earth.
Surface air pressure (p_{atm})	Pa	The pressure (force per unit area) of the atmosphere at the surface of land.
Land Surface Temperature	K	Surface temperature of 0-5 cm depth soil profile.

Dry-Delayed vs Wet-delay Systems

These systems are supported by moisture influx from deeper horizons, necessitating the decoupling of surface moisture with subsurface moisture dynamics. Such coupling is most likely to prevail in mixed forests and native prairies. On the contrary, wet-delayed systems incorporate regions with delayed transfer of increased SM to an increase in ET. These regions are most likely energy limited and are typically found at higher latitudes such as the cold deserts of Siberia.

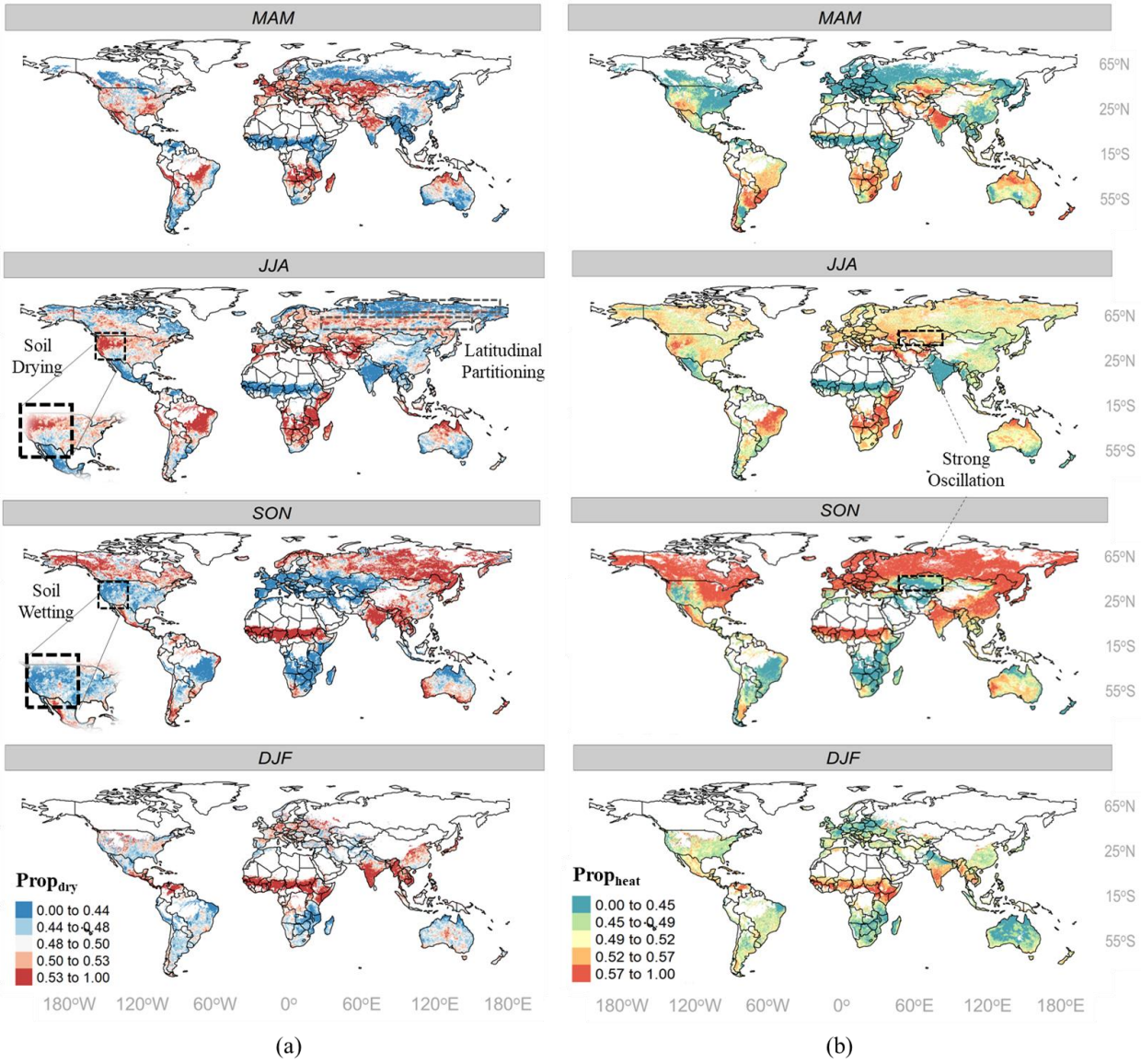

Figure S1. Global seasonal maps of **(a)** proportional duration spent by the pixel in SM drying (SM_{AIF} < 0) or SM wetting (SM_{AIF} > 0), and **(b)** proportional duration spent by the pixel in

atmosphere heating ($ET_{AIF} < 0$) or cooling ($ET_{AIF} > 0$) for four seasons, namely, March through May—MAM, June through August—JJA, September through November—SON, and December through February—DJF. The color sequential follows a quantile division of data points. Missing/masked data are represented in white color.

Table S3. Statistical summary for seasonal Wasserstein distance, WD (**-**) across hydroclimates (IQR - Interquartile Range, SD - Standard Deviation, SE - Standard Error).

Climate	WD Median	WD IQR	WD Mean	WD SD	WD SE
Super Humid	0.806	0.172	0.834	0.147	0.002
Humid	0.993	0.351	1.017	0.229	0.002
Temperate	1.112	0.370	1.111	0.253	0.001
Arid	0.983	0.427	1.025	0.281	0.002
Hyper Arid	0.766	0.201	0.812	0.183	0.001

Seasonal Slope Factor (γ)

To compute the seasonal slope factor (γ), we compared two different methods – (a) quantile regression, (b) piecewise linear regression. Quantile regression divided the time series of a location based on four quantiles (i.e., 25th, 50th, 75th, 100th percentile) while piecewise regression discretized the data based into chunks of 3 months. However, the resulting raster's from both the methods did not have much difference, hence we selected piecewise linear regression for representing γ due to its conceptual proximity with the definition of "seasonality" (i.e., MAM, JJA, SON, DJF) used in the study.

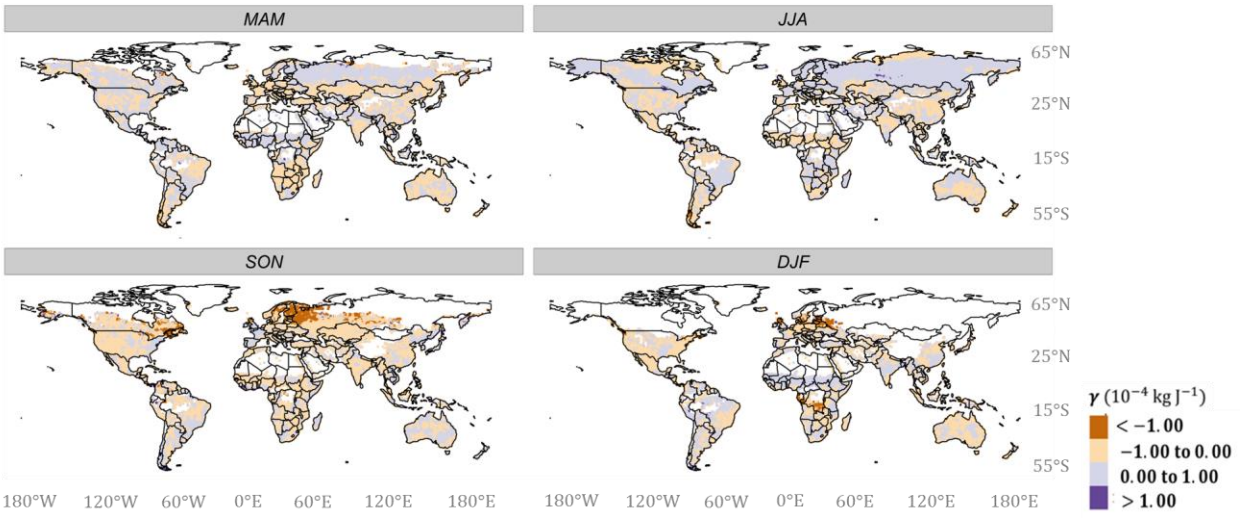

Figure S2. Global maps of seasonal slope factor, γ expressed in kg J^{-1} for four seasons, namely, March through May—MAM, June through August—JJA, September through November—SON, and December through February—DJF, computed using piecewise linear regression. Missing/masked data are represented in white color.

Relative time (τ/τ_0)

Due to discretization of γ, the resulting dimensionless quantity (τ/τ_0) might have few outliers which needs to be removed from further analysis. For example, if $\gamma \to 0$, $\tau/\tau_0 \to \infty$; such large outliers are impractical and were discarded from further analysis. Hence, values beyond 95th percentile were flagged out (i.e., values > 10000 were set equal to *NA*). Furthermore, it is important to note that as τ/τ_0 approaches zero (i.e., $\tau/\tau_0 \approx 0$ or $\tau_0 \gg \tau$), it physically represents the case where effective conductivity (K_{eff}) is very low or effective resistance (r_{eff}) is very high. This is visible (Fig. S3) in energy limited regions of Northern Eurasia and North America in the season of JJA, while regions with highest perturbations in atmospheric conditions, reflect the most variations in τ/τ_0.

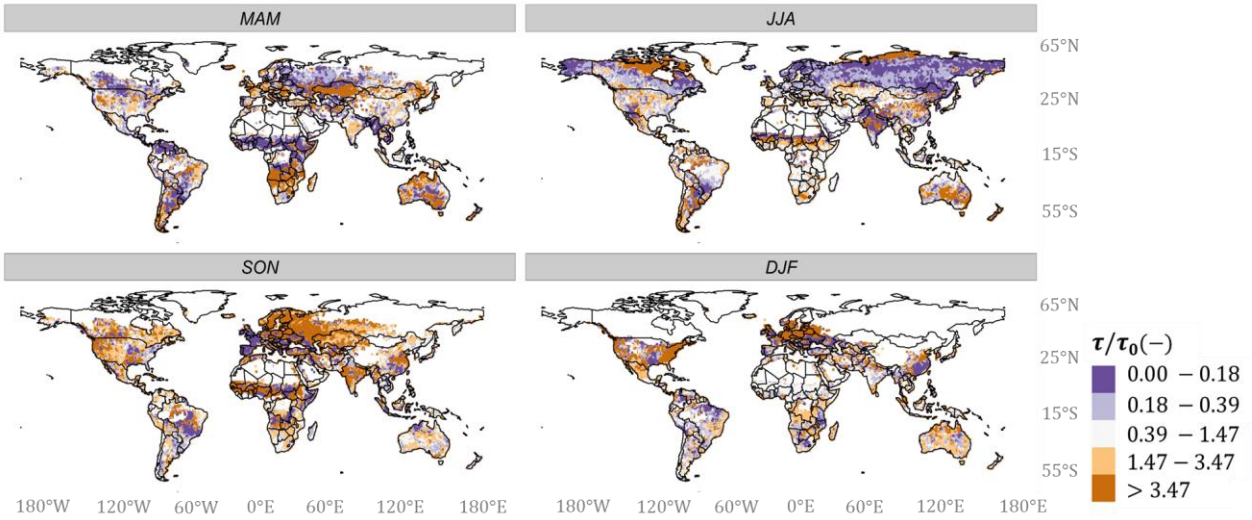

Figure S3. Global maps of relative time (τ/τ_0) for four seasons, namely, March through May—MAM, June through August—JJA, September through November—SON, and December through February—DJF. The color sequential follows a quantile division of data points. Missing/masked data are represented in white color.

Memory timescale (τ)

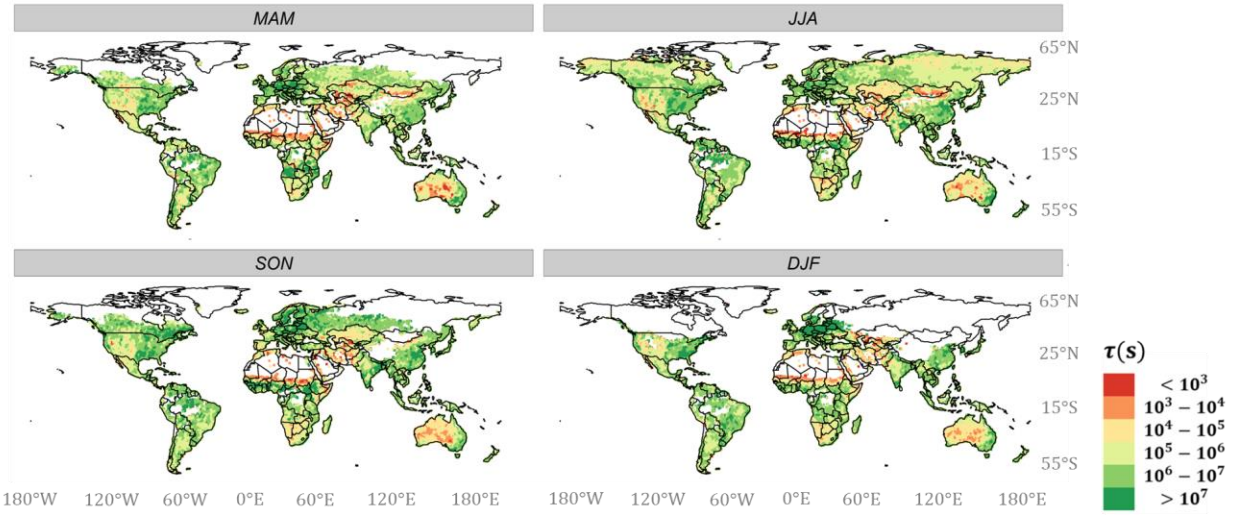

Figure S4. Global maps of memory timescale (τ), expressed in secs, for four seasons, namely, March through May—MAM, June through August—JJA, September through November—SON, and December through February—DJF. Missing/masked data are represented in white color.

Table S4. Statistical summary for seasonal entropy production, Σ^* (10^{-6} J m^{-2} K^{-1}**)** across hydroclimates (IQR - Interquartile Range, SD - Standard Deviation, SE - Standard Error).

Climate	Σ* Median	Σ* IQR	Σ* Mean	Σ* SD	Σ* SE
Super Humid	24.200	6.670	24.300	5.250	0.0793
Humid	20.800	6.490	21.100	4.880	0.0422
Temperate	18.900	6.110	19.000	4.770	0.0212
Arid	14.000	8.530	13.800	5.680	0.0256
Hyper Arid	3.340	2.780	4.140	2.840	0.0186

Table S5. Statistical summary for seasonal entropy production, Σ^* (10^{-6} J m^{-2} K^{-1}**)** across terrestrial ecosystems (IQR - Interquartile Range, SD - Standard Deviation, SE - Standard Error).

IGBP	Σ* Median	Σ* IQR	Σ* Mean	Σ* SD	Σ* SE
Forests	21.100	5.980	21.400	4.600	0.029
Savannas	18.600	7.280	18.300	6.440	0.031
Croplands	14.900	8.210	14.500	5.640	0.040
Shrublands	14.100	15.000	12.400	7.950	0.047
Grasslands	10.100	9.630	11.100	6.230	0.029
Barren	4.240	13.000	8.4500	7.750	0.195

Table S6. Dissipative energy barriers (Δe, 10^{-6} J m^{-2} K^{-1}) between terrestrial ecosystems computed as the difference between median entropy thresholds (Σ^* Median from Table 5).

	Forests	**Savannas**	**Croplands**	**Shrublands**	**Grasslands**	**Barren**
Forests	0.000					
Savannas	2.400	0.000				
Croplands	6.200	3.700	0.000			
Shrublands	7.000	4.500	0.800	0.000		
Grasslands	11.000	8.500	4.800	4.000	0.000	
Barren	16.860	14.360	10.660	9.860	5.860	0.000